

See discussions, stats, and author profiles for this publication at: <https://www.researchgate.net/publication/242187583>

# Monte Carlo simulations of free chains in end-linked polymer networks

ARTICLE *in* THE JOURNAL OF CHEMICAL PHYSICS · JULY 2001

Impact Factor: 2.95 · DOI: 10.1063/1.1379573

---

CITATIONS

16

---

READS

14

## 3 AUTHORS:



**Nisha Gilra**

ZS Associates

7 PUBLICATIONS 98 CITATIONS

SEE PROFILE



**Athanassios Z Panagiotopoulos**

Princeton University

199 PUBLICATIONS 6,714 CITATIONS

SEE PROFILE



**Claude Cohen**

Cornell University

135 PUBLICATIONS 2,625 CITATIONS

SEE PROFILE

# Monte Carlo simulations of free chains in end-linked polymer networks

Nisha Gilra

*School of Chemical Engineering, Cornell University, Ithaca, New York 14853*

Athanasios Z. Panagiotopoulos<sup>a)</sup>

*Institute for Physical Science and Technology and Department of Chemical Engineering,  
University of Maryland, College Park, Maryland 20742*

Claude Cohen

*School of Chemical Engineering, Cornell University, Ithaca, New York 14853*

(Received 20 December 2000; accepted 24 April 2001)

The structural properties of end-linked polymer networks prepared in the presence of inert linear chain solvent were investigated with Monte Carlo simulations using the three-dimensional bond fluctuation model on a simple cubic lattice. Networks of 50-mer precursor chains were prepared in a solvent of 50-mer inert linear chains with a series of concentrations and two ratios,  $r$ , of cross-link sites to chain ends. The networks were formed under both stoichiometric ( $r=1$ ) and optimal ( $r=1.2$ ) conditions for minimizing the network imperfections and soluble material and maximizing the elastic material. A maximum is observed in the fraction of elastic material at small degrees of dilution and is explained in terms of entanglement effects. The conformational behavior of a small concentration of linear 50-mer probe chains trapped in end-linked networks of mesh sizes ranging from 10- to 50-mer was also studied. The radius of gyration of the linear chains was found to decrease with decreasing mesh size of the host network, in agreement with a theoretical scaling relationship; but the magnitude of the effect is small. © 2001 American Institute of Physics.  
[DOI: 10.1063/1.1379573]

## I. INTRODUCTION AND BACKGROUND

When a polymer network is cross-linked in the presence of a solvent, the resulting network topology and macroscopic properties, such as the modulus and swelling behavior, can be significantly altered.<sup>1-3</sup> This occurs because the microscopic structure including network defects (such as loops and pendent structures) and entanglements have been changed. In particular, when a network is cross-linked in solution, the degree of entanglement present in the melt is decreased.<sup>2,4</sup> Recent experiments by Sivasailam and Cohen<sup>5</sup> of end-linked poly(dimethylsiloxane) (PDMS) networks with varying amounts of unreactive linear PDMS indicate that as the fraction of unreactive linear chains is increased, the modulus decreases, because the number of trapped entanglements decreases. Molecular dynamics simulations of end-linked polymer networks were performed by Kenkare *et al.*<sup>6</sup> in which the network was formed at a low volume fraction that was increased after the cure by growing the monomer diameter. They suggested that this method of network formation was identical to the experimental technique of cross-linking in the presence of solvent, where the solvent was considered to be vacant space in the simulation cell. They reported that networks prepared at low volume fractions had fewer chain entanglements than networks formed at high volume fractions.

At small concentrations, free linear polymer chains can also act as probes to elucidate structural details of a polymer network. For example, linear chains have been used as

probes in deformed polymer networks to determine elastic chain alignment.<sup>7-12</sup> Also, the conformational behavior of free linear chains trapped in polymer networks can be compared with the theory of polymer chains in random media.<sup>13-15</sup> This theory predicts that when the obstacle density,  $\rho$ , is sufficiently high, the chains start to shrink from their unperturbed dimensions such that their radius of gyration,  $R_g$ , scales according to  $R_g^{-1} \sim \rho$ .<sup>14</sup> If the obstacles are considered to correspond to cross-links in a polymer network, then  $\rho \sim 1/N_c$  and the predicted scaling law becomes  $R_g^{-1} \sim N_c^{-1}$ . Experimentally, Liu *et al.*<sup>16</sup> studied the conformation of linear polystyrene chains trapped in polystyrene networks using small-angle neutron scattering. They determined that the  $R_g$  of linear chain with degree of polymerization  $N_1$  was a function of the mesh size,  $N_c$ , of the network. For mesh sizes larger than  $N_1$  ( $N_c > N_1$ ),  $R_g$  did not change appreciably. While for mesh sizes smaller than  $N_1$  ( $N_c < N_1$ ),  $R_g$  was found to decrease with decreasing mesh size and obeyed  $R_g^{-1} \sim N_c^{-1}$ , in agreement with the theoretical predictions. The expansion (or contraction) of the polymer chain relative to its Gaussian state can be described by an expansion factor defined as  $\alpha = R_g/R_g^0$ , where  $R_g^0$  is the unperturbed radius of gyration of the linear chain in the melt.<sup>16</sup> The scaling relation between  $\alpha$  and  $N_c$  can then be stated as  $\alpha^{-1} \sim N_c^{-1}$ .

Computer simulation is a powerful method for studying polymer network systems because a well-characterized network system can be created and its molecular structure can be readily determined. In this paper, Monte Carlo simulations of two types of network systems are presented. The first system is one where the network is formed in the presence of

<sup>a)</sup>Current address: Department of Chemical Engineering, Princeton University, Princeton, New Jersey 08544. Electronic mail: azp@princeton.edu

inert linear chain solvent that is modeled explicitly. The network structural properties are presented as a function of the degree of dilution, or fraction of inert linear chains to reactive precursor chains. The second system is composed of a small amount of linear probe polymer chains that are trapped in a polymer network. The conformational behavior of the probe linear chains are presented as a function of network mesh size.

## II. SIMULATION METHODOLOGY

Monte Carlo simulations of polymer networks cured in the presence of solvent and linear polymer chains trapped in polymer networks were performed in the framework of the bond fluctuation model on a three-dimensional simple cubic lattice.<sup>17,18</sup> The simulation method presented here is an extension of the method used in a previous study<sup>19</sup> of networks without free chains. Periodic boundaries were imposed in the  $x$  and  $y$  directions and hard walls were placed in the  $z$  direction. Both of the network systems were created by randomly inserting the linear chains in the simulation cell and then randomly adding the precursor polymer chains and cross-links. The resulting polymer melts ( $\phi \approx 0.45$ – $0.48$ ) were equilibrated using monomer and cross-link displacement moves. Additionally, the unreactive linear chains were equilibrated using cut and regrowth moves.<sup>20,21</sup> During the cure, the networks were allowed to form using displacement moves and the cut and regrowth move was no longer used to sample different unreactive linear chain configurations due to its nonphysical nature.

The simulation details of the networks prepared in the presence of linear chain solvent are as follows. The systems were formed with 50-mer precursor polymer chains and 50-mer linear unreactive chains. These simulations were performed on a  $95 \times 95 \times 95$  cubic lattice. The networks were then allowed to cure in the presence of the unreactive linear chain diluent. Both networks with a stoichiometric ratio ( $r = 1$ ) and a ratio at which network defects are minimized ( $r_{\text{opt}} = 1.2$ )<sup>19</sup> were considered. Each system was equilibrated for approximately  $2.9 \times 10^5$  Monte Carlo step per repeat unit (MCS/RU), where a repeat unit is considered to be either a monomer or a cross-link. The cure period was  $4.1 \times 10^5$  MCS/RU for the 10% and 20% diluted networks,  $5.3 \times 10^5$  MCS/RU for the 30% diluted networks, and  $5.8 \times 10^5$  MCS/RU for the 40% and 50% diluted networks. These values of MCS/RU were chosen as the number of Monte Carlo steps beyond which the soluble fraction and network imperfections ceased changing significantly.<sup>19</sup> The cure period was identical for network systems with different  $r$  values and the same degree of dilution. The network imperfections, fraction of soluble material, and fraction of elastic material were determined using an algorithm presented previously.<sup>19</sup>

For the system of probe chains trapped in polymer networks, the systems studied consisted of ten 50-mer linear probe chains in 10-, 20-, 35-, and 50-mer polymer networks cured under stoichiometric ( $r = 1$ ) conditions. This translates to a free chain volume fraction of approximately 3.9% for each of these systems. The simulation box had dimensions of  $60 \times 60 \times 60$ . The  $R_g$  of the linear probe chains was deter-

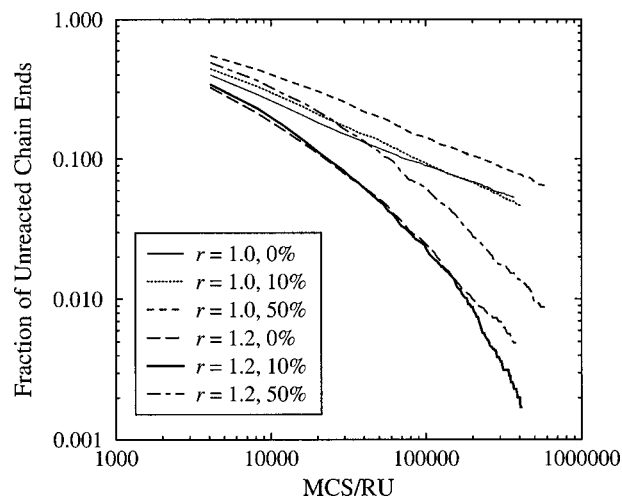


FIG. 1. Fraction of unreacted chain ends vs MCS/RU.

mined before and after the cure. After the cure, the network system was re-equilibrated in the same manner as was implemented before the cure. The 10-mer system was equilibrated for roughly  $3.7 \times 10^4$  MCS/RU before and after the cure, while the 20-, 35-, and 50-mer systems were equilibrated for approximately  $7.7 \times 10^4$  MCS/RU steps before and after the cure. The cure was approximately  $3.0 \times 10^5$  MCS/RU for the 10-mer system,  $4.6 \times 10^5$  MCS/RU for the 20-mer and 35-mer systems, and  $6.2 \times 10^5$  MCS/RU for the 50-mer system.

## III. RESULTS AND DISCUSSION

### A. Networks prepared in a solvent of linear chains

The structure of the networks is described by the fraction of unreacted chain ends, the fraction of soluble material,  $w_{\text{sol}}$ , the fraction of pendent material,  $w_{\text{pend}}$ , the fraction of single-chain loops,  $w_{\text{loops}}$ , and the fraction of elastic material,  $w_{\text{elast}}$ .<sup>19</sup> These parameters are calculated with respect to the total number of reactive precursor chains, and do not take into account the unreactive linear chains.

The evolution of the fraction of unreacted chain ends as the cure progresses is shown in Fig. 1. Each curve is the average of four independent simulations. Curves for zero dilution, which were determined previously,<sup>19</sup> are plotted on the same graph for comparison. In addition to the curves for zero dilution, only the evolution of the fraction of unreacted chain ends for the networks cured at 10% and 50% dilution are shown for purposes of clarity. The networks prepared under stoichiometric conditions follow the expected behavior because the fraction of unreacted chain ends decay as a function of  $t^{-0.5}$  at intermediate times.<sup>22</sup> For networks with  $r = 1.2$ , the decay of chain ends is faster than for the  $r = 1.0$  networks, indicating that the cure is occurring more rapidly for these networks. Furthermore, the degree of dilution affects the rate at which the cure takes place. For networks with both  $r = 1.0$  and  $r = 1.2$ , a degree of dilution of 10% causes the cure to accelerate compared to the networks that were prepared neat, whereas a degree of dilution of 50% impedes the cure. Also, the fraction of unreacted chain ends of networks with both  $r = 1.0$  and  $r = 1.2$  with 20%–40% free chains lie in between the curves for 0% and 50% dilu-

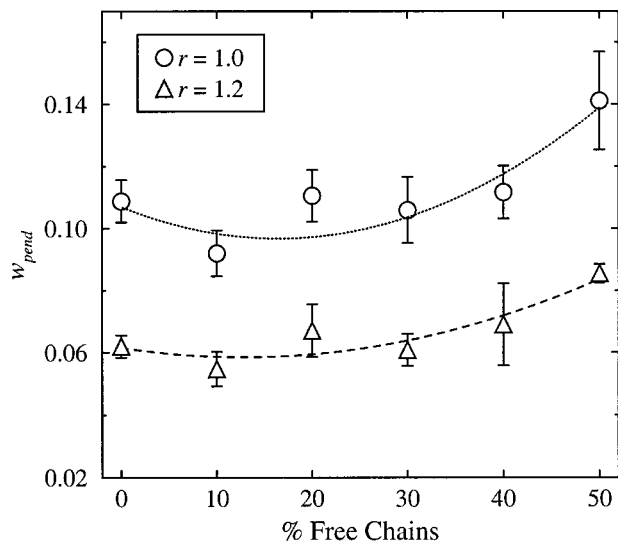


FIG. 2. Fraction of pendent material vs degree of dilution. Broken lines are guides for the eye.

tion. Thus, an accelerated cure is observed for the networks formed at 10% dilution for networks with both  $r=1.0$  and  $r=1.2$ .

Furthermore, the network structural parameters were evaluated as a function of degree of dilution. In each case, the structural parameters were taken at a constant MCS/RU that is identical for both  $r=1.0$  and  $r=1.2$  for each degree of dilution of the network. It was determined that the  $w_{sol}$  for networks with both  $r=1.0$  and  $r=1.2$  remained approximately constant with  $w_{sol}=0.0097\pm0.0011$  for  $r=1.0$  and  $w_{sol}=0.0038\pm0.0011$  for  $r=1.2$ . Additionally, in Figs. 2–4,  $w_{pend}$ ,  $w_{loops}$ , and  $w_{elast}$  are shown as a function of degree of dilution. In these plots, the dashed and dotted lines are guides for the eye.

Figure 2 shows the fraction of pendent material vs degree of dilution. The value of  $w_{pend}$  for the  $r=1.2$  networks is consistently lower than for the  $r=1.0$  networks. In addi-

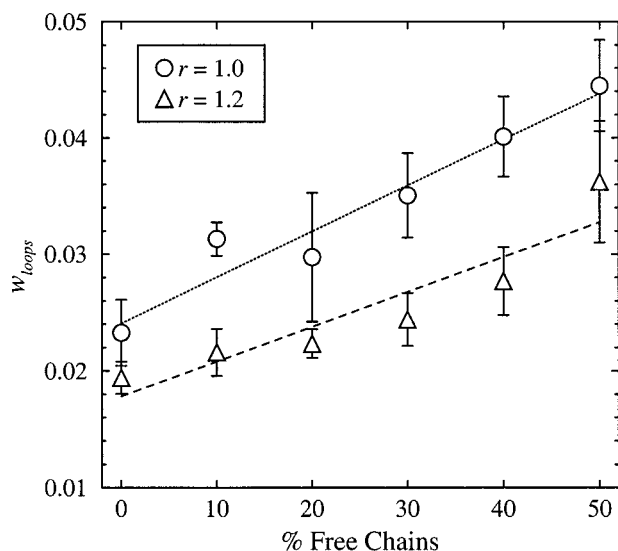


FIG. 3. Fraction of single-chain network loops vs degree of dilution. Broken lines are guides for the eye.

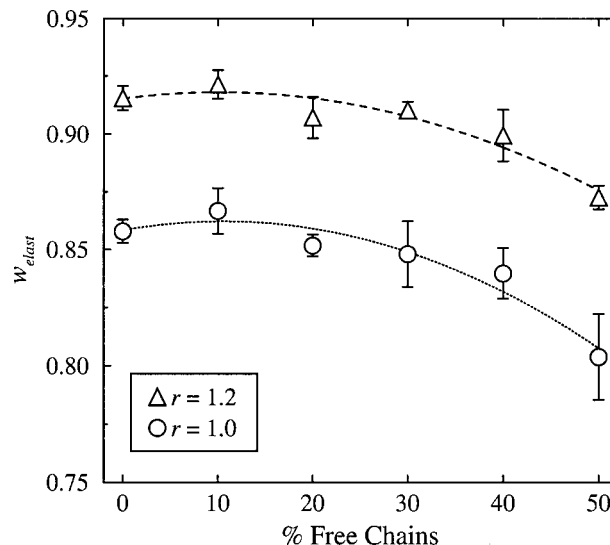


FIG. 4. Fraction of elastic material vs degree of dilution. Broken lines are guides for the eye.

tion, for both series of networks, the networks cured at 10% dilution appear to have the lowest fraction of pendent material while the networks cured at 50% dilution have the highest fraction of pendent material. This behavior may be occurring because the networks cured at 10% dilution had the highest extent of reaction indicating that, in this case, more pendent structures became part of the elastic network.

The behavior of the fraction of single-chain network loops as a function of degree of dilution is shown in Fig. 3. The fraction of loops increases with degree of dilution. Also, there are fewer loops in the networks with  $r=1.2$  than in the networks with  $r=1.0$ . The fraction of loops ranges from 2.3% to 4.4% for the networks with  $r=1.0$  and from 1.9% to 3.6% for the networks with  $r=1.2$ . There are fewer loops in the networks with  $r=1.2$  because the small excess of cross-links favors bond formation between chain ends and unreacted cross-link sites. Also, the values of  $w_{loops}$  increase with degree of dilution because the presence of the excess unreactive chains makes it less probable for an unreacted chain end to find an unsaturated cross-link other than the one with which it is already connected at its other end.

Figure 4 presents the fraction of elastic material as a function of degree of dilution. The fraction of elastic material is determined from<sup>19</sup>

$$w_{elast} = 1 - w_{sol} - w_{pend} - w_{loops}. \quad (1)$$

The  $w_{elast}$  of the  $r=1.0$  networks is always lower than that of the  $r=1.2$  networks. This result is expected from our previous results<sup>19</sup> for the 50-mer neat networks where the network properties are optimal at  $r=1.2$ . We found that the network properties are optimized at  $r=1.2$  for all degrees of dilution studied. This is consistent with experimental observations that the optimal value of  $r$  is not affected by the degree of dilution.<sup>5</sup> There is a slight maximum in  $w_{elast}$  for each of the two  $r$  values cured at 10% dilution. The strongest effect on  $w_{elast}$  appears to be from the fraction of pendent material and the fraction of single-chain loops. The fraction of single-chain loops increases with increasing degree of dilution,

while the fraction of pendent material exhibits a minimum at 10% dilution. Also, the magnitude of the fraction of pendent material (5.5%–14%) is considerably higher than the fraction of single-chain loops (1.9%–4.4%). Thus, at low (but not zero) degrees of dilution, the lower fraction of pendent material overcomes the effect of the increase of loops and maximizes the fraction of elastic material. At high degrees of dilution, both pendent structures and loops increase and cause the fraction of elastic material to decrease. The networks cured at 10% dilution had the highest extent of reaction at the end of the cure, which correlates with the decrease in the fraction of pendent material in these networks.

This behavior suggests that a small amount of solvent molecules enhance the progress of the cure. A possible explanation for this behavior is as follows. The entanglement length for linear chains in the bond fluctuation model at  $\phi \approx 0.46$ –0.48 is estimated to be  $N_e \approx 38$ .<sup>18,23</sup> The chain length of both the precursor polymer and the diluent polymer is greater than the entanglement length. This indicates that there are entanglements present in the melt. During the cure in the presence of a small fraction of the unreactive chains, only entanglements between reactive chains are trapped. Entanglements pertaining to unreactive chains can be released during the cure. The release of these entanglements, in turn, may increase the ability of unreacted chain ends to connect with unsaturated cross-links, and increase the extent of reaction. Larger fractions of the unreactive chains, however, increase the distance between unreacted chain ends and unsaturated cross-links on the network and decrease the number of elastic chains. These two opposing effects may lead to the optimal condition observed at the low degree of dilution.

### B. Probe linear chains in networks

The conformational behavior of probe chains was investigated with ten 50-mer probe chains in polymer networks with mesh sizes of 10-, 20-, 35-, and 50-mer. Each simulation was run four times in order to get estimates of the statistical uncertainty. The cut and regrow move coupled with the displacement moves allowed for better sampling than just displacement moves. The results for the expansion factor,  $\alpha$ , as a function of mesh size,  $N_c$ , are shown as  $\alpha^{-1}$  vs  $N_c^{-1}$  in Fig. 5. The decrease in  $\alpha$  with decreasing mesh size indicates that the size of polymer chains does deviate from the unperturbed dimensions in the melt. The maximum decrease in  $\alpha$  observed is approximately 6% for the 50-mer probe chains in the 10-mer network.

The  $\alpha$  values for  $N_c = 10, 20$ , and 35 confirm the scaling relationship  $\alpha^{-1} \sim N_c^{-1}$  within the accuracy of the data. The effect of the network mesh size on the free chain size is small, which is contrary to earlier neutron scattering data<sup>24</sup> that showed a large effect on chain size for mesh sizes smaller than the radius of gyration of the inert chain. Our simulation results are consistent, however, with more recent neutron scattering data<sup>25</sup> showing a rather negligible effect. The earlier results are now suspected to be due to microphase separation in these samples.

Additionally, in Fig. 5, the datum point for  $N_c = 50$  ( $N_c^{-1} = 0.02$ ) does not fall at  $\alpha = 1$  (where  $R_g = R_g^0$ ), instead

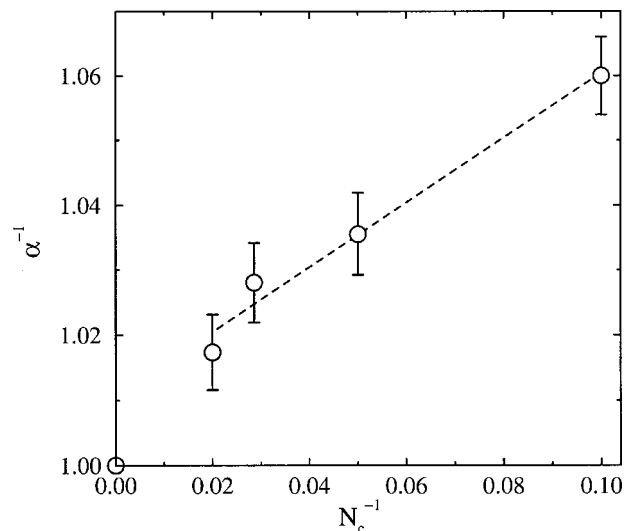


FIG. 5.  $\alpha^{-1}$  vs  $N_c^{-1}$  for the linear probe chains trapped in the polymer networks. The dashed line represents a linear fit of the data for  $N_c^{-1} \geq 0.02$ .

it appears to continue the trend established by the data at  $N_c = 10, 20$ , and 35. As noted previously, the entanglement length under our conditions is  $N_e \approx 38$ . Therefore, these results suggest that entanglements present in the 50-mer networks act to reduce the mesh size. Consequently, the  $\alpha$  value of the linear probe chains in the 50-mer networks falls in the regime of  $\alpha^{-1} \sim N_c^{-1}$  of the lower  $N_c$  networks and not near  $\alpha = 1$ . It is expected that as the value of  $N_c$  increases,  $\alpha^{-1}$  would level off at a value larger than unity when the properties of the networks become dominated by the trapped entanglements. Such simulations were not attempted because they would require significantly more computational resources. Nonetheless, the observed effect of  $N_c^{-1}$  on  $\alpha^{-1}$  is expected to be similar to the effect of  $N_c^{-1}$  on the elastic modulus observed both experimentally<sup>26</sup> and by molecular dynamics simulations.<sup>27</sup> Also, if inert chains with chain lengths less than the entanglement length ( $N_e \approx 38$ ) were to be considered, the entanglement effect observed with the 50-mer inert chains would disappear and data such as those in Fig. 5 would go through the origin. Studies of larger inert chain size would be worthwhile but also would require more computing capabilities than we currently have.

### IV. CONCLUSIONS

The structural properties of end-linked polymer networks prepared from 50-mer precursor chains in the presence of varying amounts of 50-mer inert linear chain solvent under stoichiometric ( $r = 1$ ) and optimal ( $r = 1.2$ ) conditions were obtained from Monte Carlo simulations. It was found that a degree of dilution of 10% results in networks that have a higher extent of reaction at the end of the cure. For all degrees of dilution, networks prepared at  $r = 1.2$  had a larger percentage of elastic chains. The fraction of soluble material was roughly independent of the degree of dilution, while the fraction of pendent material showed a slight minimum at 10% dilution, and the fraction of single-chain loops attached to the network increased with increasing degree of dilution.



These three components then caused the fraction of elastic material to have a slight maximum at 10% dilution for both  $r$  values studied. Curing the network in the presence of a small amount of linear chain solvent may release some of the entanglements present in the 50-mer network and increase the extent of reaction. Curing the network in the presence of larger amounts of solvent, however, makes it more difficult for unreacted chain ends to connect with unsaturated cross-links during the given cure period. These competing effects may explain why there is an optimum condition at the small degree of dilution.

The radius of gyration of 50-mer linear probe chains in networks of precursor chains ranging from 10- to 50-mer was determined. The maximum reduction of the radius of gyration was calculated to be approximately 6% for the 50-mer probe polymers in the 10-mer network, indicating that the polymer chains contracted only slightly in the confined environment. The expansion factor was found to obey the theoretical scaling relation  $\alpha^{-1} \sim N_c^{-1}$  in the range of  $N_c$  values examined. Trapped entanglements were found to affect the "effective" mesh size of the networks.

## ACKNOWLEDGMENT

Financial support for this work was provided by the Polymers Program of the National Science Foundation, under Grant Nos. DMR-9706066 and 0078863.

<sup>1</sup>P. Flory, *Polymer Chemistry* (Cornell University Press, Ithaca, 1953).

<sup>2</sup>J. Mark and B. Erman, *Rubberlike Elasticity: A Molecular Primer* (Wiley-Interscience, New York, 1988).

<sup>3</sup>M. Llorente and J. Mark, *J. Chem. Phys.* **71**, 682 (1979).

<sup>4</sup>K. Dušek and W. Prins, *Adv. Polym. Sci.* **6**, 1 (1969).

<sup>5</sup>K. Sivasailam and C. Cohen, *J. Rheol.* **44**, 897 (2000).

<sup>6</sup>N. Kenkare, S. Smith, C. Hall, and S. Khan, *Macromolecules* **31**, 5861 (1998).

<sup>7</sup>P. Sotta, B. Deloche, J. Herz, A. Lapp, D. Durand, and J.-C. Rabadeux, *Macromolecules* **20**, 2769 (1987).

<sup>8</sup>M. Depner, B. Deloche, and P. Sotta, *Macromolecules* **27**, 5192 (1994).

<sup>9</sup>J. Gao and J. Weiner, *Macromolecules* **24**, 5179 (1991).

<sup>10</sup>M. Brereton and M. Ries, *Macromolecules* **29**, 2644 (1996).

<sup>11</sup>C. Ylitalo, J. Zawada, G. Fuller, V. Abetz, and R. Stadler, *Polymer* **33**, 2949 (1992).

<sup>12</sup>P. Sotta, P. Higgs, M. Depner, and B. Deloche, *Macromolecules* **28**, 7208 (1995).

<sup>13</sup>A. Baumgärtner and M. Muthukumar, *J. Chem. Phys.* **87**, 3082 (1987).

<sup>14</sup>S. Edwards and M. Muthukumar, *J. Chem. Phys.* **89**, 2435 (1988).

<sup>15</sup>M. Muthukumar, *J. Chem. Phys.* **90**, 4594 (1989).

<sup>16</sup>X. Liu, B. Bauer, and R. Briber, *Macromolecules* **30**, 4704 (1997).

<sup>17</sup>H.-P. Deutsch and K. Binder, *J. Chem. Phys.* **94**, 2294 (1991).

<sup>18</sup>W. Paul, K. Binder, D. Heermann, and K. Kremer, *J. Phys. II* **1**, 37 (1991).

<sup>19</sup>N. Gilra, C. Cohen, and A. Panagiotopoulos, *J. Chem. Phys.* **112**, 6910 (2000).

<sup>20</sup>D. Frenkel and B. Smit, *Understanding Molecular Simulation* (Academic, San Diego, 1996).

<sup>21</sup>J. Siepmann and D. Frenkel, *Mol. Phys.* **75**, 59 (1992).

<sup>22</sup>G. Grest, K. Kremer, and E. Duering, *Europhys. Lett.* **19**, 195 (1992).

<sup>23</sup>H. Trautenberg, J.-U. Sommer, and D. Görtz, *J. Chem. Soc., Faraday Trans.* **91**, 2649 (1995).

<sup>24</sup>R. Briber, X. Liu, and B. Bauer, *Science* **268**, 395 (1995).

<sup>25</sup>N. Gilra, C. Cohen, R. Briber, B. Bauer, R. Hedden, and A. Panagiotopoulos, *Macromolecules* (submitted).

<sup>26</sup>S. Patel, S. Malone, C. Cohen, J. Gillmor, and R. Colby, *Macromolecules* **25**, 5241 (1992).

<sup>27</sup>E. Duering, K. Kremer, and G. Grest, *J. Chem. Phys.* **101**, 8169 (1994).